



Cite this: *RSC Adv.*, 2017, 7, 29103

Synthesis and antiproliferative activity of 2-aryl-4-(3,4,5-trimethoxybenzoyl)-1,2,3-triazol derivatives as microtubule-destabilizing agents†

Dongjie Feng,^a Yue Wu,^a Hao Wang,^a Zhaoshi Bai,^b Defa Wang,^a Daiying Zuo,^b Kai Bao,^{*c} Yingliang Wu^{*b} and Weige Zhang^{id} ^{*a}

A series of 2-aryl-4-(3,4,5-trimethoxybenzoyl)-1,2,3-triazols were designed as analogs of substituted methoxybenzoyl-aryl-thiazole (SMART) under the consideration of geometric features. The target compounds were synthesized *via* concise and efficient processes including microwave-assisted cyclization, and were evaluated for their antiproliferative activity against three human cancer cell lines. Most compounds exhibited moderate antiproliferative activity with IC₅₀ values in the micromolar to sub-micromolar range. Tubulin polymerization and immunofluorescence studies demonstrated that (*Z*)-**9a** was a potent microtubule-destabilizing agent and disrupted the polymerization dynamics. Moreover, (*Z*)-**9a** significantly induced accumulation of cells in the G2/M phase and caused microtubule destabilization. Molecular modeling studies showed that (*Z*)-**9a** probably binds to the colchicine site of tubulin.

Received 6th March 2017
Accepted 9th May 2017

DOI: 10.1039/c7ra02720f

rsc.li/rsc-advances

Introduction

Microtubules, a vital part of the cytoskeleton, play a crucial role in mitosis.¹ Disturbing microtubule arrangement and rearrangement, a dynamic equilibrium process, has been proved to be useful in the development of anticancer therapeutics.² Microtubule targeted agents can be classified into two major types: (1) microtubule-stabilizing agents, including taxanes and epothilones that stimulate tubulin polymerization; (2) microtubule-destabilizing agents, including vinca alkaloids and colchicine (**1**, Fig. 1) that inhibit tubulin polymerization.³

Given the success of the taxanes and vinca alkaloids,⁴ which have established tubulin as a valid target in cancer therapy, research efforts have been focusing on the development of targeted agents to the colchicine site of microtubules, known as colchicine binding site inhibitors (CBSIs).⁵ During the past decades, a large number of CBSIs have been reported,⁶ such as combretastatin A-4 (CA-4 **2**, Fig. 1), 4-substituted methoxybenzoyl-aryl-thiazole (SMART **3**, Fig. 1) and 2-aryl-4-benzoyl-imidazole (ABI **4**, Fig. 1).^{7–9} SMART, a basic three ring (A, B and C) scaffold based on the ring geometry, demonstrates potent antiproliferative activity. Moreover, a range of further

structural diversification molecules derived from the three rings has been developed to affect tubulin polymerization.¹⁰ In our previous study, a set of SMART analogs (**5**, Fig. 1) with the oxadiazole moiety as B-ring were reported to exhibit promising antiproliferative activities.¹¹

1,2,3-Triazole has gained enormous interest due to their broad spectrum of pharmaceutical and therapeutic applications.^{12,13} Furthermore, this heterocycle has a high dipole moment and is capable for hydrogen bonding, which could be favorable in the binding to biomolecular targets.¹⁴ A 1,2,3-

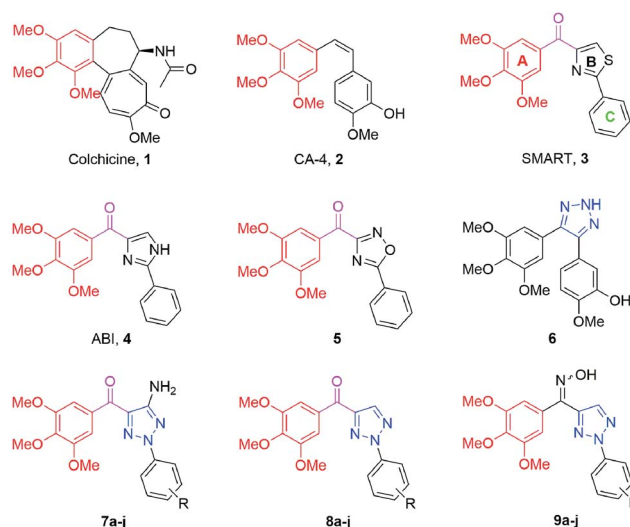


Fig. 1 Structures of reported CBSIs and designed new CBSIs.

^aKey Laboratory of Structure-Based Drug Design and Discovery, Ministry of Education, Shenyang Pharmaceutical University, 103 Wenhua Road, Shenhe District, Shenyang 110016, China. E-mail: zhangweige2000@sina.com

^bDepartment of Pharmacology, Shenyang Pharmaceutical University, 103 Wenhua Road, Shenhe District, Shenyang 110016, China. E-mail: yingliang_1016@163.com

^cWuyi College of Innovation, Shenyang Pharmaceutical University, 103 Wenhua Road, Shenhe District, Shenyang 110016, China. E-mail: baokai@syphu.edu.cn

† Electronic supplementary information (ESI) available: Experimental details. See DOI: 10.1039/c7ra02720f



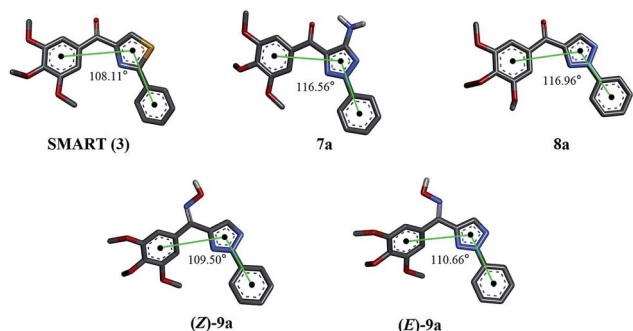


Fig. 2 Optimized structures of SMART and the target compounds **7a**, **8a**, **(Z)-9a** and **(E)-9a**. Black points represent the geometric centers of A, B and C rings, respectively.

triazol-based CA-4 analog (**6**, Fig. 1) was found to display potent antiproliferative and antitubulin activities.¹⁵

In this study, we envisaged an optimization effort around the bioisosteric B ring of SMART by replacing the thiazole ring with triazole. We hypothesized that the degree of the angle between the geometric centers of A, B and C rings ($\angle ABC$) is important for the activity of SMART and its derivatives (Fig. 2). Thus, to investigate the similarity between the designed compounds and SMART, density functional theory (DFT) calculation was applied in our case for the molecule design.^{16–18} Computational results showed the similar values of $\angle ABC$ for **(Z)-9a** and SMART, which were 109.50° and 108.11°, respectively. Therefore, a series of 2-aryl-4-(3,4,5-trimethoxybenzoyl)-1,2,3-triazole derivatives (**7–9**) were designed and the effects of substitutions on the C5 position of the triazole ring and changing the carbonyl linker into oxime were evaluated.

Results and discussion

Chemistry

The synthetic routes for 2-aryl-4-(3,4,5-trimethoxybenzoyl)-1,2,3-triazole derivatives (**7–9**) are outlined in Scheme 1. The starting material methyl 3,4,5-trimethoxybenzoate (**10**) was converted into the 3-oxo-3-(3,4,5-trimethoxyphenyl)propanenitrile (**11**) by

Table 1 The optimization of conditions for the preparation of compound **7a**

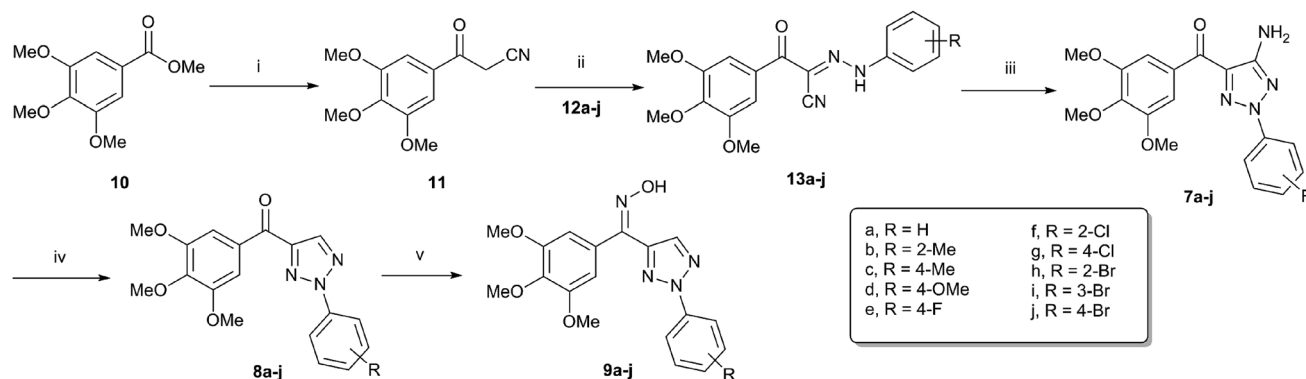
Entry	Heating	Temp (°C)	Time (min)	Yield ^a (%)
1	Oil bath	110	30 min	32
2	Oil bath	110	60 min	52
3	Oil bath	110	120 min	65
4	Oil bath	110	240 min	75
5	Oil bath	110	360 min	82
6	MW ^b	110	5 min	74
7	MW	130	5 min	81
8	MW	160	5 min	86
9	MW	160	7 min	93
10	MW	160	9 min	93

^a Isolated yield. ^b MW: microwave.

using sodium hydride and acetonitrile in THF.¹⁹ Coupling the diazonium salt of different aromatic amines (**12a–j**) with compound **11** afforded the corresponding hydrazone derivatives **13a–j**.²⁰

Under conventional heating conduction, the reaction of **13a** with hydroxylamine hydrochloride in the presence of sodium acetate to generate **7a** suffered from long reaction time and low yields (entries 1–5).²¹ As a useful tool in organic synthesis, microwave irradiation could generally accelerate the reaction rate and improve the product's yield.^{22–24} When microwave irradiation was incorporated into synthesis of **7a**, we found that the reaction rate was greatly improved. We systematically screened the influence of reaction temperature and time on the yield of **7a** under microwave conditions. As shown in Table 1, the optimized condition was confirmed to be microwave irradiation at 160 °C for 7 min (entry 9). Accordingly, all of the cyclized products **7a–j** were obtained smoothly with good to excellent yields 81–93%.

Subsequently, the amino group was removed using isoamyl nitrite in anhydrous THF under reflux conditions to yield the corresponding compounds **8a–j**,²⁵ which were then converted into oxime isomers (**9a–j**) under excess amount of hydroxylamine hydrochloride and sodium acetate by refluxing in anhydrous ethanol for 2 h.²⁶



Scheme 1 Reagents and conditions: (i) CH₃CN, NaH (70%), THF, reflux, 3 h; (ii) NaOAc, EtOH/H₂O, 0 °C, 1 h; (iii) NH₂OH·HCl, CH₃COONa, DMF, 160 °C, MW, 7 min. (iv) Isopropyl nitrite, THF, reflux, 1 h; (v) NH₂OH·HCl, CH₃COONa, EtOH, reflux, 2 h.



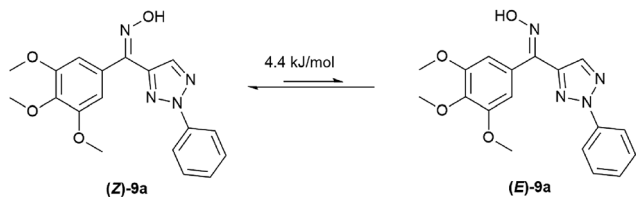


Fig. 3 Calculation of (Z/E)-9a tautomerism by DFT.

It is worth to note that there are two configurations for compounds **9a–9j** (*Z* and *E*) and the isomer mixtures were evaluated without separation in our study due to the *Z/E* tautomerism even at room temperature. Generally, the ratio of two isomers were obtained by HPLC analysis. In addition, DFT calculation of **9a** showed that *Z*-isomer should be the predominant one in the mixture (Fig. 3).

Biological evaluation

In vitro antiproliferative activity. The synthesized compounds (**7–9**) were investigated for their ability to inhibit cancer cells proliferation by the MTT method using three human carcinoma cell lines (gastric adenocarcinoma SGC-7901 cells, lung adenocarcinoma A549 cells and fibrosarcoma HT-1080 cells). The results were compared with SMART (**3**) and ABI (**4**) as the positive controls (Table 2). Of the enlisted compounds, almost all of the target compounds displayed moderate antiproliferative activity against different cancer cells with IC_{50} values in the micromolar to sub-micromolar range, which indicated the potential of the triazole ring. Among them, (**Z**)-**9a** showed the best antiproliferative activity against the SGC-7901 cell lines with IC_{50} value of $0.12 \pm 0.02 \mu\text{M}$, which was less cytotoxic than SMART ($IC_{50} = 0.019 \pm 0.008 \mu\text{M}$) but higher cytotoxic than ABI ($IC_{50} = 0.81 \pm 0.08 \mu\text{M}$). Compounds **7a–j** possessing an amino group at the C5 position of B ring were found to be more potent for A549 and HT-1080 cell lines, compared with the corresponding C5 unsubstituted compounds **8a–j**. Interestingly, the oxime linkage compounds **9a–j** were slightly better than carbonyl linkage compounds **8a–j**, which was in accorded with the calculational result that value of $\angle ABC$ in **9a** was closer to SMART than that of **7a** and **8a**. Furthermore, substitutions on C ring of the tested compounds (**7h–j**, **8h–j**, **9h–j**) exhibited an order of potency being *para* > *meta* > *ortho*-substituted in generally, and the types of substituted groups had no significant influence on antiproliferative activity.

In order to elucidate selectivity of compounds to cancer cell lines and non-cancer cell lines, we further investigated the effect of three compounds with high antiproliferative activity (**7a**, **7j**, (**Z**)-**9a**) toward normal fibroblasts L929 cells. Results are presented in Table 3. The selectivity indexes SI_A (for SGC-7901 cell line), SI_B (for A549 cell line) and SI_C (for HT-1080 cell line) were calculated. The higher selectivity index means higher therapeutic safety margin. (**Z**)-**9a** showed apparent selectivity to three cancer cell lines and normal fibroblasts L929 cells. Surprisingly, both **7a** and **7j** displayed very slight effect on L929 cells, which mean these compounds have a higher selectivity than (**Z**)-**9a**.

Table 2 *In vitro* antiproliferative activities of the target compounds (**7–9**) on three human carcinoma cell lines

Compound	IC_{50} (μM) \pm SD ^a		
	SGC-7901	A549	HT-1080
7a	0.35 \pm 0.02	0.28 \pm 0.04	0.70 \pm 0.03
7b	5.6 \pm 0.4	8.1 \pm 0.9	9.3 \pm 1.1
7c	3.3 \pm 0.2	0.26 \pm 0.02	0.41 \pm 0.05
7d	1.3 \pm 0.1	3.4 \pm 0.4	0.38 \pm 0.04
7e	1.8 \pm 0.07	2.8 \pm 0.2	0.28 \pm 0.02
7f	9.3 \pm 0.8	5.3 \pm 0.4	1.5 \pm 0.1
7g	0.70 \pm 0.05	1.6 \pm 0.1	0.24 \pm 0.01
7h	16.2 \pm 1.5	10.1 \pm 1.2	3.2 \pm 0.2
7i	0.48 \pm 0.02	1.8 \pm 0.2	2.4 \pm 0.2
7j	0.35 \pm 0.04	0.58 \pm 0.06	0.14 \pm 0.02
8a	0.87 \pm 0.09	7.1 \pm 0.6	5.2 \pm 0.8
8b	3.4 \pm 0.4	8.6 \pm 0.6	11.4 \pm 1.2
8c	1.5 \pm 0.2	7.8 \pm 0.7	4.3 \pm 0.2
8d	1.51 \pm 0.09	6.3 \pm 0.5	7.9 \pm 0.9
8e	2.9 \pm 0.3	6.7 \pm 0.8	2.4 \pm 0.3
8f	6.1 \pm 0.6	19.2 \pm 3.1	35.8 \pm 8.3
8g	1.8 \pm 0.2	3.7 \pm 0.4	0.68 \pm 0.8
8h	3.0 \pm 0.4	11.0 \pm 1.0	9.8 \pm 1.6
8i	2.4 \pm 0.2	10.4 \pm 1.1	8.2 \pm 0.7
8j	0.92 \pm 0.07	2.6 \pm 0.2	1.8 \pm 0.1
(Z)- 9a	0.12 \pm 0.02	0.52 \pm 0.3	0.34 \pm 0.4
(E)- 9a	0.61 \pm 0.05	1.23 \pm 0.07	0.98 \pm 0.1
9a ^c	0.19 \pm 0.04	0.71 \pm 0.05	0.52 \pm 0.06
9b ^c	4.9 \pm 0.3	7.2 \pm 0.7	16 \pm 1.4
9c ^c	0.32 \pm 0.04	2.4 \pm 0.3	0.54 \pm 0.05
9d ^c	0.47 \pm 0.06	0.31 \pm 0.03	6.1 \pm 0.7
9e ^c	0.42 \pm 0.04	2.1 \pm 0.2	2.1 \pm 0.3
9f ^c	3.1 \pm 0.2	6.8 \pm 0.4	37.9 \pm 6.2
9g ^c	0.38 \pm 0.06	1.6 \pm 0.09	0.49 \pm 0.02
9h ^c	1.7 \pm 0.1	12.1 \pm 2.0	41.3 \pm 6.4
9i ^c	1.3 \pm 0.2	10.2 \pm 0.9	8.5 \pm 0.7
9j ^c	0.69 \pm 0.05	0.85 \pm 0.06	0.83 \pm 0.06
SMART (3) ^b	0.019 \pm 0.008	0.029 \pm 0.009	0.028 \pm 0.016
ABI (4) ^b	0.81 \pm 0.08	0.98 \pm 0.11	0.15 \pm 0.05

^a IC_{50} : concentration of the compound (μM) producing 50% cell growth inhibition after 72 h of drug exposure, as determined by the MTT assay. Each experiment was carried out in triplicate. ^b Used as a positive control. ^c Used as mixture without separation.

Table 3 *In vitro* antiproliferative activities of **7a**, **7j** and (**Z**)-**9a** on normal fibroblasts L929 cells

Compound	L929	SI_A^a	SI_B^b	SI_C^c
7a	>100	>285.7	>357.1	>142.9
7j	45.9 \pm 3.2	131.1	79.1	327.9
(Z)- 9a	3.8 \pm 0.5	31.7	7.3	11.2

^a $SI_A = IC_{50}(\text{L929})/IC_{50}(\text{SGC-7901})$. ^b $SI_B = IC_{50}(\text{L929})/IC_{50}(\text{A549})$. ^c $SI_C = IC_{50}(\text{L929})/IC_{50}(\text{HT-1080})$.

Tubulin polymerization. With the goal of investigating the functionary mechanism on (**Z**)-**9a**, the effects of (**Z**)-**9a** on the tubulin polymerization were assessed *in vitro*. CA-4 (**2**), one of well-known CBSIs, and Taxol were applied as the positive



and negative controls, respectively. (**Z**)-**9a** caused a concentration-dependent inhibition of tubulin assembling (Fig. 4). The inhibitory activity of (**Z**)-**9a** ($IC_{50} = 5.02 \mu\text{M}$) towards tubulin polymerization was slightly weaker than the positive control CA-4 (**2**). The tubulin data suggested that (**Z**)-**9a** exerted similar influence on microtubule depolymerization as CA-4.

Immunofluorescence studies. To investigate the anti-proliferative effect of (**Z**)-**9a** was derived from interactions with tubulins, SGC-7901 cancer cells were treated with (**Z**)-**9a** at 0.12 μM for 24 h and the cellular microtubule structures were visualized by indirect immunofluorescence using an anti- α -tubulin monoclonal antibody. Data in Fig. 5 indicated that compound (**Z**)-**9a** inhibited microtubule assembly and disrupted cytoskeleton similarly to CA-4 (**2**).

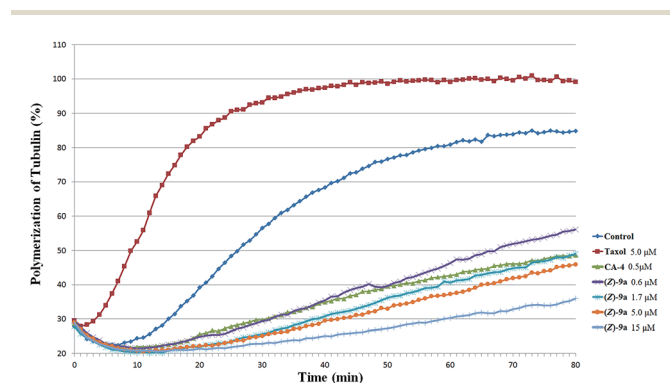


Fig. 4 Effects of (**Z**)-**9a** on tubulin polymerization. Tubulin had been pre-incubated for 1 min with (**Z**)-**9a** at 0.6 μM , 1.7 μM , 5 μM and 15 μM , CA-4 (**2**) at 0.5 μM , taxol at 5 μM or vehicle DMSO.

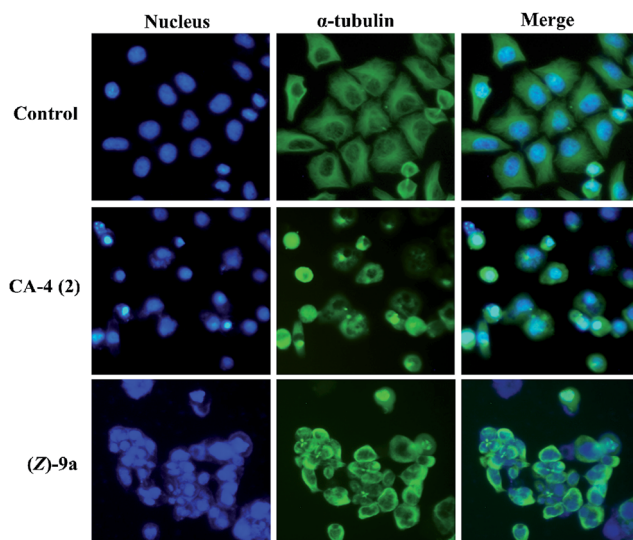


Fig. 5 (**Z**)-**9a** and CA-4 (**2**) induced depolymerization of the microtubule networks of SGC-7901 cancer cells. Untreated cells (control) and cells treated with CA-4 or (**Z**)-**9a** for 24 h, were fixed and stained with anti- α -tubulin-FITC specific antibodies followed by DAPI. Microtubules and unassembled tubulin are shown in green, and nuclei, which were stained with DAPI, are shown in blue.

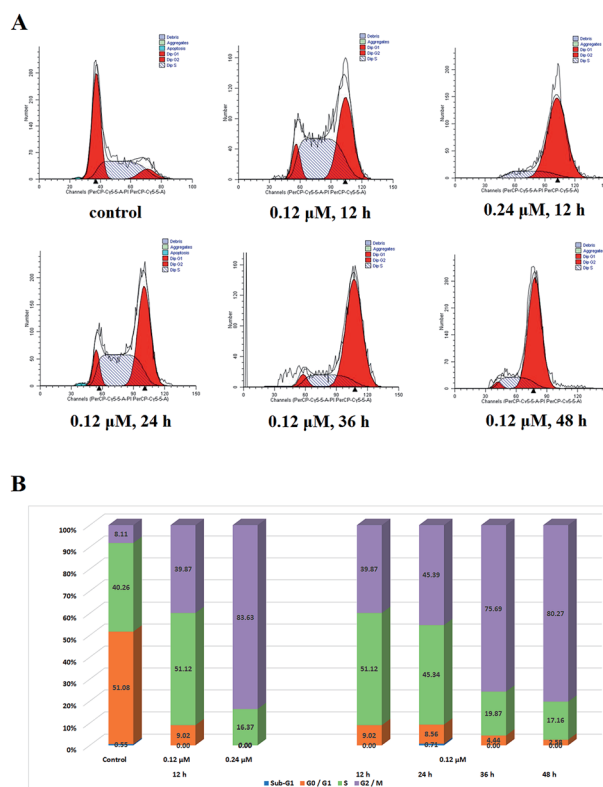


Fig. 6 Effects of (**Z**)-**9a** on cell mitosis. (A) Cell cycle distribution of SGC-7901 cancer cells treated with different concentrations of (**Z**)-**9a**. (B) The statistical graph of cell cycle distribution.

Cell cycle analysis. The cell growth inhibitory potency of the tested compounds prompted us to evaluate their effects on the cell mitosis. For cell cycle progression analysis, the effect of the (**Z**)-**9a** at various concentrations on cell cycle progression was investigated in SGC-7901 cells *via* flow cytometry. As shown in Fig. 6, (**Z**)-**9a** arrested efficiently the cell cycle progression in G2/M phase, increasing the percentage of cells in G2/M phase in a concentration-dependent manner and time-dependent manner by 40–84% and 40–80%, respectively.

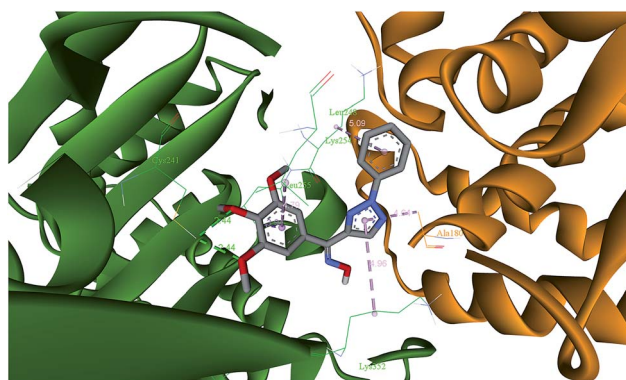


Fig. 7 The binding mode between the (**Z**)-**9a** and the α/β tubulin subunits. Location of (**Z**)-**9a** at the interface of α/β tubulin subunits (α -tubulin, yellow; β -tubulin, green). Binding mode between (**Z**)-**9a** and amino acid residues near colchicine site. The green lines represent hydrogen bonds. The pink lines represent hydrophobic interaction.



Molecular modeling study. To investigate the possible binding of target compounds to the colchicine site of tubulin, the *Z*-isomer of compound **9a**, as a predominant one in the mixture, was investigated by using CDOCKER program in Discovery Studio 3.0 software.²⁷ The docking obtained that the pose of (*Z*)-**9a** was tightly embedded into the interface of α/β tubulin subunits (Fig. 7). In the binding model, the binding orientations of (*Z*)-**9a** adopted a twisted geometry, which may be the key for its bioactivity. The two oxygen atoms of the 3,4,5-trimethoxy of (*Z*)-**9a** contributed to the hydrogen bonding interactions ($O\cdots HeN$: 2.44 Å) with the sulfhydryl group of β -CYS 241, which were consistent with other colchicine site agents reported by Massarotti *et al.*²⁸ The docking study was a beneficial complement and explanation to the above tubulin polymerization and immunofluorescence studies.

Conclusion

A series of 2-aryl-4-(3,4,5-trimethoxybenzoyl)-1,2,3-triazols characterized by a carbonyl/oxime linker, combined with/without amino substituent on the C5 position of the triazole ring, were developed under the strategy of the bioisosteric replacement of B ring of SMART. The target compounds displayed moderate antiproliferative activity against three human carcinoma cell lines. Among them, (*Z*)-**9a** exhibited best antiproliferative activity against the SGC-7901 cell lines with IC_{50} value of $0.12 \pm 0.02 \mu M$. Mechanism of action studies confirmed that (*Z*)-**9a** was a microtubule-destabilizing agent that induced the accumulation of cells in the G2/M phase and caused cell apoptosis. Structure–activity relationship between **7**, **8** and **9** indicated that $\angle ABC$ might be a considerable factor for design of SMART analogs. (*Z*)-**9a** was discovered as the most potent compound and further structural optimization and activity test will be reported in the future.

Experimental section

Chemistry

All reagents were commercially available and were used without further purification. The silica gel plate (HSGF-254) and silica gel (H, 200–300 mesh) from Yantai Jiangyou silicone Development Co., Ltd. was used for preparative TLC and column chromatography, respectively. Visualization was made with UV light (254 nm and 365 nm). Melting points were tested with Micro-Melting point apparatus (X-4, Shanghai jing science instrument Co., Ltd.) and were uncorrected. Mass spectra (MS) were obtained from Agilent Co. Ltd. on an Agilent 1100-si mass spectrometer with an electrospray ionization source. ¹H-NMR and ¹³C-NMR spectra were measured in CDCl₃ or d₆-DMSO with TMS as the internal reference on a Bruker AVANCE spectrometer operating at 400 MHz or 600 MHz (¹H at 400 or 600 MHz, ¹³C at 100 MHz). HPLC (HPLC-LC-20AT, Shimadzu) using SPD-20A UV as the detector, C18 (4.6 × 250 mm, 0.45 μm) as HPLC analysis column. Method A: gradient: 60% methanol in water as mobile elution, flow rate: 1.0 mL min⁻¹; method B: gradient: 80% methanol in water as mobile elution, flow rate: 1.0 mL min⁻¹. The microwave reactions were carried out in

a single mode cavity microwave synthesizer (CEM Corporation, NC, USA).

General synthetic procedures for 3-oxo-3-(3,4,5-trimethoxyphenyl)propanenitrile (**11**)

Mixed methyl 3,4,5-trimethoxybenzoate (5.34 g, 23.6 mmol) with NaH (47.2 mmol, 1.62 g) in boiling tetrahydrofuran (20 mL) and then followed by dropwise addition of solution of acetonitrile (23.6 mmol, 0.98 g, 1.4 mL) in tetrahydrofuran (1 mL). After refluxing for 3 h the reaction was entirely finished (TLC control). Then the mixture was cooled to room temperature and diluted by water. The precipitated sodium salt was filtered and washed with diethylether. After the evaporation of the solvent, HCl (1 mol L⁻¹) was added to acidize the compound to pH 2 and the solid was obtained, giving pale yellow solid, yield 84%. The crude **11** was utilized directly for the upcoming step without any extra purification.

General synthetic procedures for 3-oxo-3-(3,4,5-trimethoxyphenyl)-2-(phenylhydrazono) propanenitrile (**13a–j**)

To a solution of the arylamine was added hydrochloric acid (5.8 mmol in 4 mL, 6 M HCl) at 0 °C, a solution of sodium nitrite (6.4 mmol, 0.44 g dissolved in 2 mL water) was added dropwise over a period of 20 min, and stirring at 0 °C for 30 min to form the corresponding aryldiazonium salt (**12a–j**). Then the resulting solution of aryldiazonium salt was dropwise added to a solution of 3-oxo-3-(3,4,5-trimethoxyphenyl)propanenitrile (1.5 g, 6.4 mmol) in ethanol mixture (10 mL) involving sodium acetate trihydrate (0.95 g, 11.6 mmol) at 0 °C. Then the mixture was stirred at room temperature for 1 h and the resulting solid was collected by filtration, washed with water and ethanol. The crude **13a–j** was utilized directly for the upcoming step without any extra purification.

General synthetic procedures for 5-amino-2-aryl-4-(3,4,5-trimethoxybenzoyl)-1,2,3-triazol (**7a–j**)

Independent mixtures of **13a–j** (1 mmol) containing hydroxylamine hydrochloride (0.35 g, 5 mmol) and anhydrous sodium acetate (0.41 g, 5 mmol) in DMF (5 mL) were stirred at irradiated in a microwave reactor for 7 min at 160 °C. The reaction mixtures were cooled to room temperature and poured into ice cold water. The formed solids were collected by filtration, washed with water. The residual crude product was purified by column chromatography on silica gel (200–300 mesh) with petroleum ether/AcOEt (v/v = 3 : 1).

5-Amino-2-phenyl-4-(3,4,5-trimethoxybenzoyl)-2H-1,2,3-triazol (7a**).** Compound **7a** was obtained from **13a** as a yellow solid (0.31 g, 93%); mp 166–170 °C; ¹H NMR (400 MHz, CDCl₃) δ 8.03 (d, *J* = 7.9 Hz, 2H), 7.83 (s, 2H), 7.49 (t, *J* = 7.6 Hz, 7.9 Hz, 2H), 7.37 (t, *J* = 7.6 Hz, 1H), 3.99 (s, 6H), 3.97 (s, 3H) ppm; ¹³C NMR (100 MHz, CDCl₃) δ 183.9, 152.9 (×2), 147.5, 143.1, 139.5, 138.8, 131.3, 129.5 (×2), 128.6, 119.2 (×2), 108.0 (×2), 61.0, 56.3 (×2) ppm; MS (ESI): [M + H]⁺ = 355.1, [M + Na]⁺ = 377.1.

5-Amino-2-(*o*-tolyl)-4-(3,4,5-trimethoxybenzoyl)-2H-1,2,3-triazol (7b**).** Compound **7b** was obtained from **13b** as a yellow solid (0.32 g, 86%); mp 185–187 °C; ¹H NMR (400 MHz, CDCl₃) δ 7.68



(s, 2H), 7.63 (d, $J = 7.6$ Hz, 1H), 7.36 (m, 3H), 3.94 (s, 3H), 3.92 (s, 6H), 2.48 (s, 3H) ppm; ^{13}C NMR (100 MHz, CDCl_3) δ 185.6, 152.8 ($\times 2$), 149.5, 143.6, 142.6, 139.1, 132.2, 132.1, 131.8, 129.1, 126.7, 125.0, 107.9 ($\times 2$), 60.9, 56.2 ($\times 2$), 19.2 ppm; MS (ESI): $[\text{M} + \text{H}]^+ = 369.1$, $[\text{M} + \text{Na}]^+ = 391.1$.

5-Amino-2-(*p*-tolyl)-4-(3,4,5-trimethoxybenzoyl)-2H-1,2,3-triazol (7c). Compound **7c** was obtained from **13c** as a yellow solid (0.33 g, 89%); mp 173–176 °C; ^1H NMR (400 MHz, CDCl_3) δ 7.90 (d, $J = 8.5$ Hz, 2H), 7.83 (s, 2H), 7.28 (d, $J = 8.5$ Hz, 2H), 3.98 (s, 6H), 3.97 (s, 3H), 2.41 (s, 3H) ppm; ^{13}C NMR (100 MHz, CDCl_3) δ 185.4, 156.5, 152.8 ($\times 2$), 142.4, 137.9, 137.2, 132.0, 131.3, 129.9 ($\times 2$), 118.5 ($\times 2$), 107.7 ($\times 2$), 61.0, 56.2 ($\times 2$), 21.0 ppm; MS (ESI): $[\text{M} + \text{H}]^+ = 369.1$, $[\text{M} + \text{Na}]^+ = 391.1$.

5-Amino-2-(4-methoxyphenyl)-4-(3,4,5-trimethoxybenzoyl)-2H-1,2,3-triazol (7d). Compound **7d** was obtained from **13d** as a yellow solid (0.31 g, 81%); mp 201–203 °C; ^1H NMR (400 MHz, CDCl_3) δ 7.94 (m, 2H), 7.82 (s, 2H), 6.99 (m, 2H), 3.98 (s, 6H), 3.96 (s, 3H), 3.86 (s, 3H) ppm; ^{13}C NMR (100 MHz, CDCl_3) δ 185.4, 159.3, 156.5, 152.8 ($\times 2$), 142.3, 133.1, 132.0, 131.1, 120.1 ($\times 2$), 114.5 ($\times 2$), 107.7 ($\times 2$), 61.0, 56.2 ($\times 2$), 55.6 ppm; MS (ESI): $[\text{M} + \text{H}]^+ = 385.1$, $[\text{M} + \text{Na}]^+ = 407.1$.

5-Amino-2-(4-fluorophenyl)-4-(3,4,5-trimethoxybenzoyl)-2H-1,2,3-triazol (7e). Compound **7e** was obtained from **13e** as a yellow solid (0.34 g, 91%); mp 193–195 °C; ^1H NMR (400 MHz, CDCl_3) δ 8.00 (m, 2H), 7.80 (s, 2H), 7.18 (m, 2H), 3.97 (s, 6H), 3.97 (s, 3H) ppm; ^{13}C NMR (100 MHz, CDCl_3) δ 185.5, 161.9 (d, $J = 246.7$ Hz), 156.6, 152.8 ($\times 2$), 142.5, 135.7, 131.8 ($\times 2$), 131.6, 120.3 (d, $J = 8.2$ Hz, $\times 2$), 116.3 (d, $J = 23.0$ Hz, $\times 2$), 107.7 ($\times 2$), 61.0, 56.2 ($\times 2$) ppm; MS (ESI): $[\text{M} + \text{H}]^+ = 373.1$, $[\text{M} + \text{Na}]^+ = 395.1$.

5-Amino-2-(2-chlorophenyl)-4-(3,4,5-trimethoxybenzoyl)-2H-1,2,3-triazol (7f). Compound **7f** was obtained from **13f** as a yellow solid (0.35 g, 90%); mp 181–184 °C; ^1H NMR (600 MHz, CDCl_3) δ 8.21 (s, 1H), 7.95 (d, $J = 8.1$ Hz, 1H), 7.82 (s, 2H), 7.48 (d, $J = 7.9$ Hz, 1H), 7.35 (t, $J = 8.0$ Hz, 1H), 3.98 (s, 6H), 3.97 (s, 3H) ppm; ^{13}C NMR (100 MHz, CDCl_3) δ 185.3, 156.4, 152.8 ($\times 2$), 142.6, 140.1, 131.9, 131.6, 130.6, 130.5, 123.0, 121.8, 116.9, 107.7 ($\times 2$), 60.9, 56.1 ($\times 2$) ppm; MS (ESI): $[\text{M} + \text{H}]^+ = 389.1$, $[\text{M} + \text{Na}]^+ = 411.1$.

5-Amino-2-(4-chlorophenyl)-4-(3,4,5-trimethoxybenzoyl)-2H-1,2,3-triazol (7g). Compound **7g** was obtained from **13g** as a yellow solid (0.34 g, 87%); mp 168–170 °C; ^1H NMR (600 MHz, CDCl_3) δ 7.90 (d, $J = 8.6$ Hz, 2H), 7.79 (s, 2H), 7.61 (d, $J = 8.6$ Hz, 2H), 3.97 (s, 9H) ppm; ^{13}C NMR (100 MHz, CDCl_3) δ 185.5, 156.5, 152.8 ($\times 2$), 138.3, 133.7, 132.5 ($\times 2$), 131.9, 131.8, 121.3, 120.0 ($\times 2$), 107.7 ($\times 2$), 61.0, 56.2 ($\times 2$) ppm; MS (ESI): $[\text{M} + \text{H}]^+ = 389.1$, $[\text{M} + \text{Na}]^+ = 411.1$.

5-Amino-2-(2-bromophenyl)-4-(3,4,5-trimethoxybenzoyl)-2H-1,2,3-triazol (7h). Compound **7h** was obtained from **13h** as a yellow solid (0.36 g, 83%); mp 153–159 °C; ^1H NMR (600 MHz, CDCl_3) δ 8.30 (s, 1H), 8.04 (d, $J = 8.0$ Hz, 1H), 7.69 (s, 2H), 7.53 (d, $J = 7.5$ Hz, 1H), 7.38 (t, $J = 8.0$ Hz, 1H), 3.98 (s, 3H), 3.96 (s, 6H) ppm; ^{13}C NMR (100 MHz, CDCl_3) δ 185.7, 156.4, 152.9, 142.6, 139.2, 134.4 ($\times 2$), 132.1, 131.8, 130.4, 128.2, 127.6, 117.5, 107.8 ($\times 2$), 60.9, 56.4 ($\times 2$), 21.9 ppm; MS (ESI): $[\text{M} + \text{H}]^+ = 433.0$.

5-Amino-2-(3-bromophenyl)-4-(3,4,5-trimethoxybenzoyl)-2H-1,2,3-triazol (7i). Compound **7i** was obtained from **13i** as

a yellow solid (0.37 g, 86%); mp 172–176 °C; ^1H NMR (600 MHz, CDCl_3) δ 7.84 (s, 2H), 7.69 (m, 1H), 7.58 (m, 1H), 7.41 (m, 2H), 3.94 (s, 9H) ppm; ^{13}C NMR (100 MHz, CDCl_3) δ 185.6, 156.3, 152.8, 142.5, 137.4, 132.1, 131.7, 131.3 ($\times 2$), 129.9, 128.2, 127.6, 127.0, 107.7 ($\times 2$), 60.9, 56.2 ($\times 2$), 21.9 ppm; MS (ESI): $[\text{M} + \text{H}]^+ = 433.0$, $[\text{M} + \text{Na}]^+ = 455.0$.

5-Amino-2-(4-bromophenyl)-4-(3,4,5-trimethoxybenzoyl)-2H-1,2,3-triazol (7j). Compound **7j** was obtained from **13j** as a yellow solid (0.40 g, 92%); mp 182–186 °C; ^1H NMR (600 MHz, CDCl_3) δ 7.96 (m, 2H), 7.79 (s, 2H), 7.46 (m, 2H), 3.97 (s, 9H) ppm; ^{13}C NMR (100 MHz, CDCl_3) δ 185.5, 156.6, 152.8 ($\times 2$), 142.6, 138.3, 132.5 ($\times 2$), 131.9, 131.8, 121.4, 120.1 ($\times 2$), 107.7 ($\times 2$), 61.0, 56.2 ($\times 2$), 21.9 ppm; MS (ESI): $[\text{M} + \text{H}]^+ = 433.0$, $[\text{M} + \text{Na}]^+ = 455.1$.

General synthetic procedures for 2-aryl-4-(3,4,5-trimethoxybenzoyl)-1,2,3-triazol (8a–j)

To a solution of compound **7a–j** (1 mmol) in anhydrous THF (5 mL) was added isopropyl nitrite (2 mmol). The original material was completely depleted after one hour refluxing. After the evaporation of the solvent, the residue was purified by column chromatography on silica gel (200–300 mesh) with petroleum ether/AcOEt (v/v = 3 : 1) or pure CH_2Cl_2 .

2-Phenyl-4-(3,4,5-trimethoxybenzoyl)-2H-1,2,3-triazol (8a). Compound **8a** was obtained from **7a** as a light yellow solid (0.27 g, 81%); mp 138–140 °C; ^1H NMR (400 MHz, CDCl_3) δ 8.42 (s, 1H), 8.16 (d, $J = 7.9$ Hz, 2H), 7.77 (s, 2H), 7.54 (dd, $J = 7.5$ Hz, 7.9 Hz, 2H), 7.44 (t, $J = 7.5$ Hz, 1H), 3.98 (s, 3H), 3.97 (s, 6H) ppm; ^{13}C NMR (100 MHz, CDCl_3) δ 185.7, 156.7, 153.0 ($\times 2$), 142.6, 139.5, 132.0, 131.8, 129.5 ($\times 2$), 128.0, 118.8 ($\times 2$), 107.9 ($\times 2$), 61.1, 56.4 ($\times 2$) ppm; MS (ESI): $[\text{M} + \text{H}]^+ = 340.1$, $[\text{M} + \text{Na}]^+ = 362.1$.

2-(*o*-Tolyl)-4-(3,4,5-trimethoxybenzoyl)-2H-1,2,3-triazol (8b). Compound **8b** was obtained from **7b** as a light yellow solid (0.29 g, 83%); mp 146–148 °C; ^1H NMR (400 MHz, CDCl_3) δ 8.45 (s, 1H), 7.76 (s, 2H), 7.67 (d, $J = 7.8$ Hz, 1H), 7.38 (m, 3H), 3.96 (s, 3H), 3.94 (s, 6H), 2.48 (s, 3H) ppm; ^{13}C NMR (100 MHz, CDCl_3) δ 183.9, 152.9 ($\times 2$), 147.4, 143.0, 139.1, 138.3, 132.4, 131.8, 131.3, 129.3, 126.8, 125.1, 107.9 ($\times 2$), 60.9, 56.2 ($\times 2$), 19.1 ppm; MS (ESI): $[\text{M} + \text{H}]^+ = 354.1$, $[\text{M} + \text{Na}]^+ = 376.1$.

2-(*p*-Tolyl)-4-(3,4,5-trimethoxybenzoyl)-2H-1,2,3-triazol (8c). Compound **8c** was obtained from **7c** as a light yellow solid (0.28 g, 80%); mp 149–152 °C; ^1H NMR (400 MHz, CDCl_3) δ 8.39 (s, 1H), 8.02 (d, $J = 8.2$ Hz, 2H), 7.77 (s, 2H), 7.33 (d, $J = 8.2$ Hz, 2H), 3.98 (s, 3H), 3.97 (s, 6H), 2.43 (s, 3H) ppm; ^{13}C NMR (100 MHz, CDCl_3) δ 184.0, 152.9 ($\times 2$), 147.3, 143.0, 138.7, 138.6, 137.3, 131.4, 130.1 ($\times 2$), 119.1 ($\times 2$), 108.0 ($\times 2$), 61.0, 56.3 ($\times 2$), 21.1 ppm; MS (ESI): $[\text{M} + \text{H}]^+ = 354.1$, $[\text{M} + \text{Na}]^+ = 376.1$.

2-(4-Methoxyphenyl)-4-(3,4,5-trimethoxybenzoyl)-2H-1,2,3-triazol (8d). Compound **8d** was obtained from **7d** as a light yellow solid (0.25 g, 69%); mp 168–172 °C; ^1H -NMR (600 MHz, CDCl_3) δ 8.69 (d, $J = 2.7$ Hz, 1H), 8.41 (s, 1H), 8.33 (dd, $J = 2.7$ Hz, 8.0 Hz, 1H), 7.75 (s, 2H), 7.27 (d, $J = 8.0$ Hz, 1H), 4.06 (s, 3H), 3.98 (s, 3H), 3.97 (s, 6H) ppm; ^{13}C NMR (100 MHz, CDCl_3) δ 183.9, 159.8, 152.9 ($\times 2$), 147.1, 142.9, 138.5, 133.1, 131.4, 120.7



($\times 2$), 114.5 ($\times 2$), 108.0 ($\times 2$), 61.0, 56.2 ($\times 2$), 55.6 ppm; MS (ESI): $[M + H]^+ = 370.1$, $[M + Na]^+ = 392.1$.

2-(4-Fluorophenyl)-4-(3,4,5-trimethoxybenzoyl)-2H-1,2,3-triazol (8e). Compound **8e** was obtained from **7e** as a light yellow solid (0.27 g, 74%); mp 158–161 °C; 1H NMR (600 MHz, $CDCl_3$) δ 8.37 (s, 1H), 8.10 (m, 2H), 7.71 (s, 2H), 7.20 (m, 2H), 3.96 (s, 3H), 3.94 (s, 6H) ppm; ^{13}C NMR (100 MHz, $CDCl_3$) δ 183.8, 162.3 (d, $J = 247.5$ Hz), 152.9 ($\times 2$), 147.5, 143.1, 138.8 ($\times 2$), 135.7 (d, $J = 2.9$ Hz), 131.2, 121.0 (d, $J = 8.3$ Hz, $\times 2$), 116.4 (d, $J = 23.2$ Hz, $\times 2$), 107.9 ($\times 2$), 60.9, 56.2 ($\times 2$) ppm; MS (ESI): $[M + H]^+ = 358.1$, $[M + Na]^+ = 380.1$.

2-(2-Chlorophenyl)-4-(3,4,5-trimethoxybenzoyl)-2H-1,2,3-triazol (8f). Compound **8f** was obtained from **7f** as a light yellow solid (0.28 g, 76%); mp 161–164 °C; 1H NMR (600 MHz, $CDCl_3$) δ 8.42 (s, 1H), 8.35 (t, $J = 1.9$ Hz, 8.1 Hz, 1H), 8.10 (m, 1H), 7.75 (s, 2H), 7.56 (m, 1H), 7.41 (t, $J = 1.9$ Hz, 8.1 Hz, 1H), 3.99 (s, 3H), 3.98 (s, 6H) ppm; ^{13}C NMR (100 MHz, $CDCl_3$) δ 183.7, 153.0 ($\times 2$), 147.8, 143.2, 140.3, 139.1, 131.5, 131.1, 130.9, 123.2, 122.5, 117.7, 108.0 ($\times 2$), 61.0, 56.3 ($\times 2$) ppm; MS (ESI): $[M + H]^+ = 374.1$.

2-(4-Chlorophenyl)-4-(3,4,5-trimethoxybenzoyl)-2H-1,2,3-triazol (8g). Compound **8g** was obtained from **7g** as a light yellow solid (0.30 g, 81%); mp 136–140 °C; 1H NMR (600 MHz, $CDCl_3$) δ 8.40 (s, 1H), 8.11 (m, 2H), 7.72 (s, 2H), 7.50 (m, 2H), 3.98 (s, 3H), 3.96 (s, 6H) ppm; ^{13}C NMR (100 MHz, $CDCl_3$): $\delta = 183.7$, 152.9, 147.6, 143.1, 138.9 ($\times 2$), 137.9, 134.3, 131.1, 129.7 ($\times 2$), 120.4 ($\times 2$), 107.9 ($\times 2$), 61.0, 56.2 ($\times 2$) ppm; MS (ESI): $[M + H]^+ = 374.1$, $[M + Na]^+ = 396.1$.

2-(2-Bromophenyl)-4-(3,4,5-trimethoxybenzoyl)-2H-1,2,3-triazol (8h). Compound **8h** was obtained from **7h** as a light yellow solid (0.30 g, 73%); mp 168–172 °C; 1H NMR (600 MHz, $CDCl_3$) δ 8.48 (s, 1H), 7.81 (d, $J = 1.1$ Hz, 1H), 7.79 (s, 2H), 7.64 (dd, $J = 7.7$ Hz, 1.6 Hz, 1H), 7.51 (m, 1H), 7.42 (td, $J = 7.7$ Hz, 1.6 Hz, 1H), 3.95 (s, 3H), 3.95 (s, 6H) ppm; ^{13}C NMR (100 MHz, $CDCl_3$) δ 183.9, 161.4, 153.0, 147.9, 143.2, 138.8, 134.7, 134.2, 131.2 ($\times 2$), 128.3, 128.0, 118.5, 108.1 ($\times 2$), 61.0, 56.4 ($\times 2$) ppm; MS (ESI): $[M + H]^+ = 418.0$, $[M + Na]^+ = 440.1$.

2-(3-Bromophenyl)-4-(3,4,5-trimethoxybenzoyl)-2H-1,2,3-triazol (8i). Compound **8i** was obtained from **7i** as a light yellow solid (0.32 g, 76%); mp 156–158 °C; 1H NMR (600 MHz, $CDCl_3$) δ 8.48 (s, 1H), 7.79 (s, 2H), 7.70 (dd, $J = 7.5$ Hz, 2.0 Hz, 1H), 7.62 (dd, $J = 7.5$ Hz, 1.6 Hz, 1H), 7.47 (m, 2H), 3.95 (s, 3H), 3.95 (s, 6H) ppm; ^{13}C NMR (100 MHz, $CDCl_3$) δ 183.9, 153.0, 148.0, 143.1, 138.8, 137.6, 131.2, 131.2 ($\times 2$), 130.8, 129.1, 127.7, 127.6, 108.0 ($\times 2$), 61.0, 56.3 ($\times 2$) ppm; MS (ESI): $[M + H]^+ = 418.0$, $[M + Na]^+ = 440.0$.

2-(4-Bromophenyl)-4-(3,4,5-trimethoxybenzoyl)-2H-1,2,3-triazol (8j). Compound **8j** was obtained from **7j** as a light yellow solid (0.33 g, 79%); mp 150–153 °C; 1H NMR (600 MHz, $CDCl_3$) δ 8.38 (s, 1H), 8.00 (d, $J = 8.0$ Hz, 2H), 7.70 (s, 2H), 7.63 (d, $J = 8.0$ Hz, 2H), 3.96 (s, 3H), 3.94 (s, 6H) ppm; ^{13}C NMR (100 MHz, $CDCl_3$) δ 183.6, 152.9 ($\times 2$), 147.6, 143.1, 138.9, 138.3, 132.6 ($\times 2$), 131.1, 122.2, 120.6 ($\times 2$), 107.9 ($\times 2$), 60.9, 56.2 ($\times 2$) ppm; MS (ESI): $[M + H]^+ = 418.0$, $[M + Na]^+ = 440.0$.

General synthetic procedures for compounds (9a–j)

An excess of hydroxylamine hydrochloride (15 mmol) was added to a solution of compound **8a–j** (1 mmol) and sodium acetate (15 mmol) in absolute ethanol (5 mL). After reacting at 80 °C for 2 h, the reaction was entirely finished (TLC control). Then the mixture was added to water (20 mL) and extracted with EtOAc (20 mL \times 3). The combined organic layers were washed with water, dried over Na_2SO_4 , and the solvent was then evaporated under reduced pressure. The residue was purified by column chromatography (petroleum ether/AcOEt = 2 : 1 as eluent) on silica gel to obtain pure product.

(*Z* + *E*)-(2-Phenyl-2H-1,2,3-triazol-4-yl)(3,4,5-trimethoxyphenyl)methanone oxime (**9a**). Compound **9a** was obtained from **8a** as a white solid (0.33 g, 94%) with a 76 : 24 mixture of *Z* and *E* isomers; mp 132–135 °C; 1H NMR (400 MHz, $CDCl_3$) (*Z* isomer): δ 9.23 (s, 1H), 8.57 (s, 1H), 8.10 (d, $J = 8.0$ Hz, 2H), 7.49 (dd, $J = 7.6$ Hz, 8.0 Hz, 2H), 7.38 (t, $J = 7.6$ Hz, 1H), 6.98 (s, 1H), 3.92 (s, 3H), 3.88 (s, 6H) ppm; (*E* isomer): δ 8.05 (d, $J = 7.9$ Hz, 2H), 7.96 (s, 1H), 7.45 (dd, $J = 7.9$ Hz, 2H), 7.35 (m, 1H), 6.86 (s, 1H), 3.94 (s, 3H), 3.86 (s, 6H) ppm; 1H NMR (600 MHz, d_6 -DMSO) (*Z* isomer): δ 12.26 (s, 1H), 8.67 (s, 1H), 8.03 (d, $J = 7.9$ Hz, 2H), 7.59 (t, $J = 7.6$ Hz, 2H), 7.45 (t, $J = 7.1$ Hz, 1H), 6.99 (s, 1H), 3.78 (s, 3H), 3.73 (s, 6H) ppm; MS (ESI): $[M + H]^+ = 355.1$, $[M + Na]^+ = 377.1$.

(*Z* + *E*)-(2-(*o*-Tolyl)-2H-1,2,3-triazol-4-yl)(3,4,5-trimethoxyphenyl)methanone oxime (**9b**). Compound **9b** was obtained from **8b** as a white solid (0.33 g, 89%) with a 92 : 8 mixture of *Z* and *E* isomers; mp 307–310 °C; 1H NMR (400 MHz, $CDCl_3$) (*Z* isomer) δ 10.30 (s, 0.6H), 8.60 (s, 1H), 7.57 (d, $J = 7.6$ Hz, 1H), 7.35 (m, 3H), 6.95 (s, 2H), 3.90 (s, 3H), 3.86 (s, 6H), 2.40 (s, 3H) ppm; (*E* isomer) δ 8.04 (s, 1H), 7.58 (m, 1H), 7.28 (m, 3H), 6.85 (s, 2H), 3.92 (s, 3H), 3.84 (s, 6H), 2.40 (s, 3H) ppm; MS (ESI): $[M + H]^+ = 369.2$.

(*Z* + *E*)-(2-(*p*-Tolyl)-2H-1,2,3-triazol-4-yl)(3,4,5-trimethoxyphenyl)methanone oxime (**9c**). Compound **9c** was obtained from **8c** as a white solid (0.34 g, 92%) with a 82 : 18 mixture of *Z* and *E* isomers; mp 142–145 °C; 1H NMR (400 MHz, $CDCl_3$) (*Z* isomer) δ 8.39 (s, 1H), 8.02 (d, $J = 8.4$ Hz, 2H), 7.77 (s, 2H), 7.33 (d, $J = 8.4$ Hz, 2H), 3.98 (s, 3H), 3.97 (s, 6H), 2.44 (s, 3H) ppm; (*E* isomer) δ 8.17 (s, 1H), 7.95 (d, $J = 8.2$ Hz, 2H), 7.30 (d, $J = 8.2$ Hz, 2H), 6.68 (s, 2H), 3.93 (s, 3H), 3.81 (s, 6H), 2.42 (s, 3H) ppm; MS (ESI): $[M + H]^+ = 369.1$, $[M + Na]^+ = 391.1$.

(*Z* + *E*)-(2-(4-Methoxyphenyl)-2H-1,2,3-triazol-4-yl)(3,4,5-trimethoxyphenyl)methanone oxime (**9d**). Compound **9d** was obtained from **8d** as a white solid (0.33 g, 87%) with a 89 : 11 mixture of *Z* and *E* isomers; mp 178–180 °C; 1H NMR (400 MHz, $CDCl_3$) (*Z* isomer) δ 9.80 (s, 1H); 8.57 (s, 1H); 8.08 (d, $J = 7.7$ Hz, 2H); 7.46 (d, $J = 7.7$ Hz, 2H); 6.97 (s, 2H); 3.93 (s, 3H); 3.88 (s, 6H), 3.48 (s, 3H) ppm; MS (ESI): $[M + H]^+ = 385.1$, $[M + Na]^+ = 407.1$.

(*Z* + *E*)-(2-(4-Fluorophenyl)-2H-1,2,3-triazol-4-yl)(3,4,5-trimethoxyphenyl)methanone oxime (**9e**). Compound **9e** was obtained from **8e** as a white solid (0.31 g, 84%) with a 78 : 22 mixture of *Z* and *E* isomers; mp 139–147 °C; 1H NMR (600 MHz, $CDCl_3$) (*Z* isomer) δ 8.40 (s, 1H), 8.14 (m, 2H), 7.73 (s, 2H), 7.23 (m, 2H), 6.66 (s, 1H), 3.98 (s, 3H), 3.97 (s, 6H) ppm; (*E* isomer)



δ 8.19 (s, 1H), 8.06 (m, 2H), 7.73 (s, 2H), 7.20 (m, 2H), 6.66 (s, 2H), 3.93 (s, 3H), 3.81 (s, 6H). ppm; MS (ESI): $[M + H]^+ = 373.1$.

(*Z* + *E*)-(2-(2-Chlorophenyl)-2*H*-1,2,3-triazol-4-yl)(3,4,5-trimethoxyphenyl)methanone oxime (**9f**). Compound **9f** was obtained from **8f** as a white solid (0.33 g, 86%) with a 84 : 16 mixture of *Z* and *E* isomers; mp 215–218 °C; ¹H NMR (600 MHz, *d*₆-DMSO) (*Z* isomer) δ 12.29 (s, 0.2H), 8.75 (s, 1H), 8.14 (m, *J* = 9.8 Hz, 2H), 7.74 (m, *J* = 8.0 Hz, 1H), 7.63 (s, 2H), 7.60 (m, 1H), 3.81 (s, 3H), 3.78 (s, 6H); (*E* isomer) δ 11.89 (s, 0.2H), 8.78 (s, 1H), 8.26 (s, 2H), 8.02 (d, *J* = 8.0 Hz, 2H), 7.67 (d, *J* = 8.0 Hz, 1H), 7.58 (m, 1H), 3.90 (s, 9H) ppm; MS (ESI): $[M + H]^+ = 389.1$, $[M + Na]^+ = 411.1$.

(*Z* + *E*)-(2-(4-Chlorophenyl)-2*H*-1,2,3-triazol-4-yl)(3,4,5-trimethoxyphenyl)methanone oxime (**9g**). Compound **9g** was obtained from **8g** as a white solid (0.35 g, 91%) with a 88 : 12 mixture of *Z* and *E* isomers; mp 184–189 °C; ¹H NMR (600 MHz, CDCl₃) (*Z* isomer) δ 8.55 (s, 1H), 8.03 (d, *J* = 8.6 Hz, 2H), 7.45 (d, *J* = 8.6 Hz, 2H), 6.94 (s, 2H), 3.91 (s, 3H), 3.86 (s, 6H) ppm; (*E* isomer) δ 8.41 (s, 1H), 8.09 (d, *J* = 8.8 Hz, 2H), 7.72 (s, 2H), 7.51 (d, *J* = 8.8 Hz, 2H), 3.98 (s, 3H), 3.96 (s, 6H) ppm; MS (ESI): $[M + H]^+ = 389.1$, $[M + Na]^+ = 411.1$.

(*Z* + *E*)-(2-(2-Bromophenyl)-2*H*-1,2,3-triazol-4-yl)(3,4,5-trimethoxyphenyl)methanone oxime (**9h**). Compound **9h** was obtained from **8h** as a white solid (0.39 g, 90%) with a 71 : 29 mixture of *Z* and *E* isomers; mp 195–198 °C; ¹H NMR (600 MHz, CDCl₃) (*Z* isomer) δ 8.65 (s, 1H), 7.73 (d, *J* = 7.5 Hz, 1H), 7.56 (d, *J* = 6.0 Hz, 1H), 7.45 (d, *J* = 7.4 Hz, 1H), 7.36 (t, *J* = 7.2 Hz, 1H), 6.96 (s, 2H), 3.88 (s, 3H), 3.86 (s, 6H) ppm; (*E* isomer) δ 8.09 (s, 1H), 7.72 (s, 1H), 7.55 (s, 1H), 7.42 (d, *J* = 7.2 Hz, 1H), 7.32 (s, 1H), 6.87 (s, 2H), 3.90 (s, 3H), 3.85 (s, 6H) ppm; MS (ESI): $[M + H]^+ = 433.0$, $[M + Na]^+ = 455.0$.

(*Z* + *E*)-(2-(3-Bromophenyl)-2*H*-1,2,3-triazol-4-yl)(3,4,5-trimethoxyphenyl)methanone oxime (**9i**). Compound **9i** was obtained from **8i** as a white solid (0.40 g, 92%) with a 82 : 18 mixture of *Z* and *E* isomers; mp 180–185 °C; ¹H-NMR (600 MHz, CDCl₃): (*Z* isomer) δ 9.23 (s, 0.6H), 8.63 (s, 1H), 7.61 (dd, *J* = 1.8 Hz, 7.57 Hz, 1H), 7.6 (dd, *J* = 1.6 Hz, 7.9 Hz, 1H), 7.43 (dd, *J* = 1.8 Hz, 7.9 Hz, 1H), 7.41 (dd, *J* = 1.6 Hz, 7.6 Hz, 1H), 6.96 (s, 2H), 3.88 (s, 3H), 3.87 (s, 6H) ppm; (*E* isomer) δ 8.49 (s, 1H), 7.79 (s, 2H), 7.70 (dd, *J* = 1.9 Hz, 7.5 Hz, 1H), 7.63 (d, *J* = 1.8 Hz, 1H), 7.47 (d, *J* = 1.9 Hz, 1H), 7.45 (d, *J* = 1.8 Hz, 1H), 3.95 (s, 3H), 3.94 (s, 6H) ppm; MS (ESI): $[M + H]^+ = 433.0$, $[M + Na]^+ = 455.1$.

(*Z* + *E*)-(2-(4-Bromophenyl)-2*H*-1,2,3-triazol-4-yl)(3,4,5-trimethoxyphenyl)methanone oxime (**9j**). Compound **9j** was obtained from **8j** as a white solid (0.40 g, 93%) with a 83 : 17 mixture of *Z* and *E* isomers; mp 201–205 °C; ¹H NMR (600 MHz, *d*₆-DMSO) (*Z* isomer) δ 12.26 (s, 1H), 8.66 (s, 1H), 8.03 (m, 2H), 7.42 (m, 2H), 6.97 (s, 2H), 3.78 (s, 6H), 3.76 (s, 3H) ppm; (*E* isomer) δ 11.83 (s, 1H), 8.27 (s, 1H), 7.95 (m, 1H), 7.47 (m, 1H), 6.86 (s, 1H), 3.73 (s, 3H), 3.72 (s, 6H) ppm; MS (ESI): $[M + H]^+ = 433.0$.

Biology

Cell line and culture conditions. The human gastric adenocarcinoma SGC-7901 cells, lung adenocarcinoma A549 cells, fibrosarcoma HT-1080 cells and normal fibroblasts L929 cells

were purchased from Shanghai Institute of Cell Resources Center of Life Science (Shanghai, China). All cells were cultured in RPMI-1640 medium (Invitrogen, USA) supplemented with 10% fetal bovine serum (FBS; Hyclone, USA), streptomycin and penicillin at 37 °C in humidified atmosphere with 5% CO₂.

Antiproliferative activity assay. The antiproliferative activity assay *in vitro* was carried out referring to the previously reported method.²⁴ **9a–j** was used without separation. (*Z*)-**9a** and (*E*)-**9a** were separated from mixture and was used immediately.

Tubulin polymerization assay. The tubulin polymerization assay was carried out referring to the previously reported method.²⁴ (*Z*)-**9a** was separated from mixture and was used immediately.

Immunofluorescence assay. The immunofluorescence assay was carried out referring to the previously reported method.²⁹ (*Z*)-**9a** was separated from mixture and was used immediately. 4',6-Diamidino-2-phenylindole (DAPI) was purchased from Sigma Chemical (St. Louis, MO, USA) and the primary α -tubulin antibody was used (Santa Cruz, CA, USA).

Cell cycle assay. The cell cycle assay was carried out referring to the previously reported method.²⁹ (*Z*)-**9a** was separated from mixture and was used immediately.

Computational assay. Geometry optimization of molecules was carried out at the B3LYP level of theory with the 6-31G(d) basis set on Gaussian 09 software package. The angles were calculated by methods of analytic geometry manually according to the coordinate data from Gaussian software. The molecular modelling studies were performed with Accelrys Discovery Studio 3.0.^{17,18} The crystal structures of tubulin complexed with DAMA-colchicine (PDB: 1SA0) was retrieved from the RCSB Protein Data Bank (<http://www.rcsb.org/pdb>).²⁷ The ligand **9a** model was optimized by molecular dynamic force field, and docked into the binding site using the CDOCKER protocol with the default settings. The image of Fig. 2 and 7 was possessed by Discovery Studio 4.5 Visualizer.

Acknowledgements

We gratefully acknowledge the National Natural Science Foundation of China (81673293, 81502932, 81602969) and State Key Laboratory of Natural Medicines and Active Substance (No. GTZK201603) for their generous financial support. This work was also supported by Program for Innovative Research Team of the Ministry of Education and Program for Liaoning Innovative Research Team in University.

References

- 1 M. A. Jordan and L. Wilson, *Nat. Rev. Cancer*, 2004, **4**, 253.
- 2 C. Dumontet and M. A. Jordan, *Nat. Rev. Drug Discovery*, 2010, **9**, 790.
- 3 E. A. Perez, *Mol. Cancer Ther.*, 2009, **8**, 2086.
- 4 Y. Lu, J. Chen, M. Xiao, W. Li and D. D. Miller, *Pharm. Res.*, 2012, **29**, 2943.
- 5 M. N. Islam and M. N. Iskander, *Mini-Rev. Med. Chem.*, 2004, **4**, 1077.



- 6 G. G. Dark, S. A. Hill, V. E. Prise, G. M. Tozer, G. R. Pettit and D. J. Chaplin, *Cancer Res.*, 1997, **57**, 1829.
- 7 G. R. Pettit, B. Toki, D. L. Herald, P. V. Pinard, M. R. Boyd, E. Hamel and R. K. Pettit, *J. Med. Chem.*, 1998, **41**, 1688.
- 8 Y. Lu, C.-M. Li, Z. Wang, C. R. Ross II, J. Chen, J. T. Dalton, W. Li and D. D. Miller, *J. Med. Chem.*, 2009, **52**, 1701.
- 9 J. Chen, Z. Wang, C. M. Li, Y. Lu, P. K. Vaddady, B. Meibohm, J. T. Dalton, D. D. Miller and W. Li, *J. Med. Chem.*, 2010, **53**, 7414.
- 10 J. Chen, S. Ahn, J. Wang, Y. Lu, J. T. Dalton, D. D. Miller and W. Li, *J. Med. Chem.*, 2012, **55**, 7285.
- 11 Q. Guan, D. Feng, Z. Bai, Y. H. Cui, D. Zuo, M. Zhai, X. Jiang, W. Zhou, K. Bao, Y. Wu and W. Zhang, *MedChemComm*, 2015, **6**, 1484.
- 12 H. C. Kolb and K. B. Sharpless, *Drug Discovery Today*, 2003, **8**, 1128.
- 13 V. D. Bock, D. Speijer, H. Hiemstra and J. H. V. Maarseveen, *Org. Biomol. Chem.*, 2007, **5**, 971.
- 14 Y. C. Duan, Y. C. Ma, E. Zhang, X. J. Shi, M. M. Wang, X. W. Ye and H. M. Liu, *Eur. J. Med. Chem.*, 2013, **62**, 11.
- 15 N. R. Madadi, N. R. Penthalala, K. Howk, A. Ketkar, R. L. Eoff, M. J. Borrelli and P. A. Crooks, *Eur. J. Med. Chem.*, 2015, **103**, 123.
- 16 A. D. Baecke, *J. Chem. Phys.*, 1993, **98**, 5648.
- 17 C. Lee, W. Yang and R. G. Parr, *Phys. Rev. B: Condens. Matter Mater. Phys.*, 1988, **37**, 785.
- 18 M. J. Frisch, G. W. Trucks, H. B. Schlegel, G. E. Scuseria, M. A. Robb, J. R. Cheeseman, J. A. Montgomery, T. Vreven, K. N. Kudin, J. C. Burant, J. M. Millam, S. S. Iyengar, J. Tomasi, V. Barone, B. Mennucci, M. Cossi, G. Scalmani, N. Rega, G. A. Petersson, H. Nakatsuji, M. Hada, M. Ehara, K. Toyota, R. Fukuda, J. Hasegawa, M. Ishida, T. Nakajima, Y. Honda, O. Kitao, H. Nakai, M. Klene, X. Li, J. E. Knox, H. P. Hratchian, J. B. Cross, V. Bakken, C. Adamo, J. Jaramillo, R. Gomperts, R. E. Stratmann, O. Yazyev, A. J. Austin, R. Cammi, J. C. Pomelli, J. W. Ochterski, P. Y. Ayala, K. Morokuma, G. A. Voth, P. Salvador, J. J. Dannenberg, V. G. Zakrzewski, S. Dapprich, A. D. Daniels, M. C. Strain, O. Farkas, D. K. Malick, A. D. Rabuck, K. Raghavachari, J. B. Foresman, J. V. Ortiz, Q. Cui, A. G. Baboul, S. Clifford, J. Cioslowski, B. B. Stefanov, G. Liu, A. Liashenko, P. Piskorz, I. Komaromi, R. L. Martin, D. J. Fox, T. Keith, M. A. Al-Laham, C. Y. Peng, A. Nanayakkara, M. Challacombe, P. M. W. Gill, B. Johnson, W. Chen, M. W. Wong, C. Gonzalez and J. A. Pople, *Gaussian 09, Revision D.01*, Gaussian, Inc., Wallingford CT, 2009.
- 19 S. Wang, Y. Yin, Y. Zhang, S. Mi, M. Zhao, P. Lv, B. Wang and H. Zhu, *Eur. J. Med. Chem.*, 2015, **93**, 291.
- 20 H. Behbehani, H. M. Ibrahim and S. Makhseed, *Heterocycles*, 2009, **78**, 3081.
- 21 L. Wu, S. Guo, X. Wang, Z. Guo, G. Yao, Q. Lin and M. Wu, *Tetrahedron Lett.*, 2015, **56**, 2145.
- 22 C. O. Kappe and D. Dallinger, *Mol. Diversity*, 2009, **13**, 171.
- 23 A. Hoz, A. Ortiz and A. Moreno, *Chem. Soc. Rev.*, 2005, **34**, 164.
- 24 Z. Wen, J. Xu, Z. Wang, H. Qi, Q. Xu, Z. Bai, Q. Zhang, K. Bao, Y. Wu and W. Zhang, *Eur. J. Med. Chem.*, 2015, **90**, 184.
- 25 T. Yang, G. Chen, Z. Sang, Y. Liu, X. Yang, Y. Chang, H. Long, W. Ang, J. Tang, Z. Wang, G. Li, S. Yang, J. Zhang, Y. Wei and Y. Luo, *J. Med. Chem.*, 2015, **58**, 6389.
- 26 Y. Lu, C.-M. Li, Z. Wang, J. Chen, M. L. Mohler, W. Li, J. T. Dalton and D. D. Miller, *J. Med. Chem.*, 2011, **54**, 4678.
- 27 R. B. Ravelli, B. Gigant, P. A. Curmi, I. Jourdain, S. Lachkar, A. Sobel and M. Knossow, *Nature*, 2004, **428**, 198.
- 28 A. Massarotti, A. Coluccia, R. Silvestri, G. Sorba and A. Brancale, *ChemMedChem*, 2012, **7**, 33.
- 29 Q. Xu, Y. Wang, J. Xu, M. Sun, H. Tian, D. Zuo, Q. Guan, K. Bao, Y. Wu and W. Zhang, *ACS Med. Chem. Lett.*, 2016, **7**, 1202.

